Association of Metallurgical Engineers of Serbia *Scientific paper*
AMES *UDC: 620.193/.197 ; 621.793/.795 ; 667.6*

COMPARATIVE STUDY ON THE CORROSION RESISTANCE OF Zn-0.2 Pb AND Zn-0.5 Sb GALVANIZED COATINGS

A. Bakhtiari*[1], H.R. Asgari[2]

[1]*Department of Materials Engineering, Isfahan University of Technology, Isfahan, Iran*
[2] *Dezful Islamic Azad University, Dezful,. Iran*

Received 18.07.2011
Accepted 10.09.2011

Abstract

In this work, The corrosion behavior of Zn-0.2 Pb and Zn-0.5 Sb galvanized coatings in 3.5 wt.% NaCl aqueous solutions was investigated using scanning electron microscopy (SEM), energy dispersive spectroscopy (EDS), electrochemical impedance spectroscopy (EIS) and Tafel extrapolation techniques. The texture of the coatings was evaluated using X-ray diffraction. All coatings were galvanized in molten zinc bath with different chemical composition. The results revealed that the corrosion mechanism of the Zn coatings with Sb content is related to the appearance of cracks due to the dissolution of the γ Zn-rich phases, while the corrosion of the Zn-0.2 Pb coating was characterized by dissolution of the coatings. Furthermore, Zn coatings with Sb show strong (00.2) basal texture component than Zn coatings with Pb. Besides, coatings with strong (00.2) basal texture component have better corrosion resistance.

Keywords: hot-dip galvanized coatings, corrosion resistance, electrochemical impedance spectroscopy technique, texture

Introduction

Hot-dipped galvanized (HDG) zinc-coated sheet steels are used in a wide variety of product applications. Zinc coatings were used in industrial field such as automobile, electrical home applications or construction due to their excellent corrosion performance [1-3]. Minor elements added to the bath for spangle formation are required to have a very limited solubility in solid zinc. In addition, these elements lower the tension of molten zinc on the sheet so that a uniform coating on the sheet is effectively achieved. Pb or Sb are usually incorporated to the zinc bath in most continuous galvanizing lines in the world. Either of these elements has advantages over the other. In

* Corresponding author. Amirreza. Bakhtiari, bakhtiari.amirreza@gmail.com

consideration of a larger spangle only, Sb may be more effective than Pb. The concentration of Sb or Pb in the zinc bath should be carefully determined since excessive or very little addition would detract from the coating properties [4-5]. Although the aim of their addition is very similar, the coating appearances and properties can be different according to the element chosen. Corrosion resistance can also be varied depending on the elements within the coating as well as surface morphologies [3-5].

The preferred crystallographic orientation (texture) is an important factor which affects the coating properties and depends strongly on external factors such as cooling rate gradient, surface conditions of steel substrate during the coating solidification process and bath chemical composition [6].

The present study deals with the corrosion behavior and texture of the zinc hot-dip coatings especially considering Pb and Sb additions.

Experimental procedure

The material tested was hot-dipped coating that was prepared on the continuous commercial production line. Samples were prepare in the dimension of 60×40×0.4mm. All the tests were carried out four times with commercially available JIS G3302 HDG steel sheets and the average of the results considered as the final report. In addition, production conditions such as rolling finishing temperature, cooling temperature, cold work percentage and annealing conditions are the same for all the specimens. Chemical composition of substrate and production parameters is shown in Tables 1 and 2, respectively.

Table 1 Chemical composition of steel substrate (wt.%)

C	*Si*	*Mn*	*P*	*S*	*Al*	*N*	**Fe**
0.027	0.004	0.222	0.007	0.004	0.058	30ppm	Bal

Table 2 Production parameters of sample

Zinc bath temperature (°C)	*Sheet thickness (mm)*	*Strip-entry temperature (°C)*	*Galvanized line speed (m/min)*	*Jet wiper distance from sheet surface (mm)*
450	0.4	466±1	100	100

Cross sections of the coatings were studied using scanning electron microscopy (SEM) electron image mode obviously equipped with EDS. Because of high sensitivity of zinc to water, absolute alcohol was used for grinding and polishing of samples. Also, polishing was performed along the Fe-Zn layers and grinding was carried out employing soft and papers. Composition of the coating layers was determined using energy dispersive spectroscopy (EDS) analysis

The crystallographic orientation of the coating was determined using X-ray diffraction (XRD) (Philips XL model 30, Cu K_α radiation, step size 0.03^0, counting time

of 1s). A 2θ scan was preformed between 20^0 and 100^0 and the integrated intensities (termed as $I_{(hk.l)}$) of several reflections were determined. It should be noted that since integrated intensities require background subtraction each $I_{(hk.l)}$ was normalized by dividing it by its structure factor or random intensity, $I^0_{(hk.l)}$, giving $I^n_{(hk.l)}$. Values of $I^0_{(hk.l)}$ were obtained from powder zinc pattern. It should be mentioned that nine values of $I^n_{(hk.l)}$, representing nine planes, were calculated but in this paper only one value of $I^n_{(hk.l)}$ is presented.

Corrosion behavior was analyzed by electrochemical impedance spectroscopy (EIS) and Tafel polarization techniques were conduced in a 3.5 wt.% NaCl solution at room temperature. A standard corrosion cell kit consisted of two graphite counter electrodes as the working electrodes and an AgCl as the reference electrode.

The volume of the electrolyte for each test was 500 ml. potentiodynamic scanning was performed by stepping the potential at a scan rate of 1 mV/s from -250 mV to 250 mV. The (EIS) experiments were performed in a frequency range of 4 mHz to 10 kHz and a sinusoidal amplitude perturbation of 5 mV rms

Results and discussion

Figure 1 shows a typical cross section of zinc coated samples; four distinct coating layers of HDG steel can be identified in this micrograph. Energy dispersive spectroscopy analysis of the coating layers indicated that coatings consisted of: γ (71.3 wt-%Zn, 28.7 wt-%Fe), δ (93.8 wt-%Zn, 6.2 wt-%Fe), ζ (95.8 wt-%Zn, 4.2 wt-%Fe) and η (98.9 wt-%Zn, 1.1 wt-%Fe).

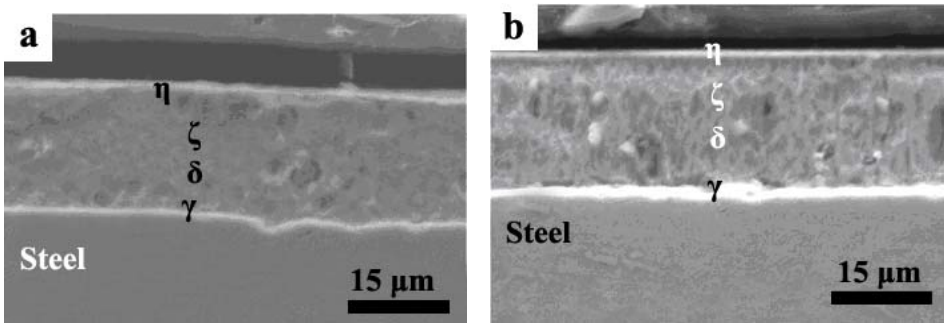

Fig 1. SEM micrographs of cross-section of samples (a. Zn-0.2 Pb; b. Zn-0.5 Sb)

Figure 2 depicts typical SEM images of the Zn coatings after the EIS tests with 5 days immersion time, revealing a surface covered with corrosion products on the surface, indicating that corrosion occurs. The cross-section SEM image of the Zn-0.2 Pb coating (Figure 2a) shows the local dissolution of the complete coating after 5 days of immersion time. However, the cross section morphology of the Zn-0.5 Sb coating after 5 days of immersion time displayed cracks from the surface down to the substrate (Figure 2b). These SEM analyses are in agreement with previous studies of the corrosion behavior of galvanized steel and galvannealed steel in aqueous NaCl solution, where the appearance of cracks were associated with the dissolution of zinc-rich phases [7-8]. Another report also shows a similar evolution of cracking of the Zn-Ni layer

during the corrosion process [6]. Finally, localized EDS analyses performed on the layer and near the cracked region of the Zn-0.5 Sb unveiled that the Sb content in the layer was about 24 at.%, while this content in the cracked region was about 55 at.%, suggesting that the Sb enrichment in the layer was associated with the dissolution of residual Zn and Zn-rich phases.

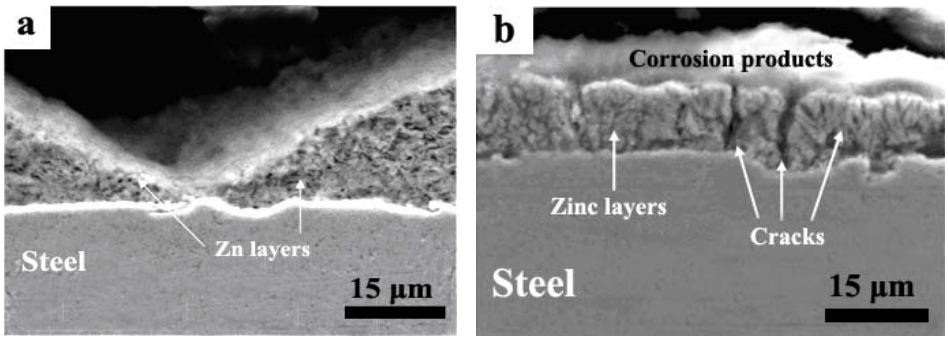

Fig 2. SEM micrographs SEM micrographs of cross-section of samples after the end of 5days of immersion time (a. Zn-0.2 Pb; b. Zn-0.5 Sb)

Figure 3 illustrates the XRD diagrams of specimens. Zn-0.2 Pb and Zn-0.5 Sb showing different texture components.

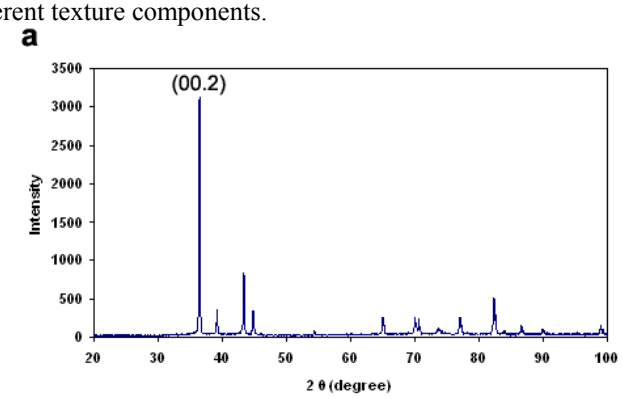

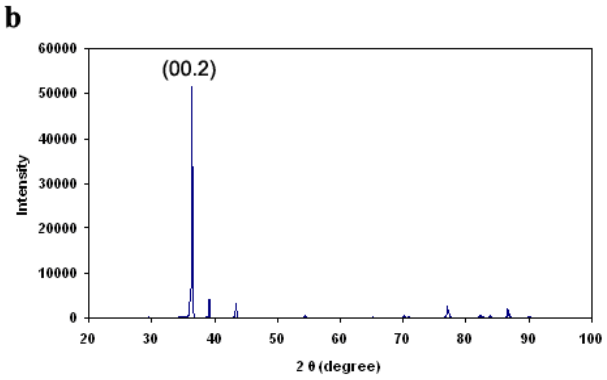

Fig. 3. XRD diagrams of samples (a) Zn-0.2 Pb and (b) Zn-0.5 Sb with different (00.2) basal texture component

It is obvious from Figure 4, that the Pb content of the zinc bath was accompanied by decrease of basal plane intensity. Although HDG zinc coatings often show a strong (00.2) basal texture component [1], in the case of Pb additions, the (00.2) basal texture component was much lower compared when Sb content was added to the zinc bath. This suggested that, when the Pb content of zinc bath is added, less nuclei of basal planes form and, consequently, less basal planes with low corrosion resistance will be formed and lower area of the surface would be covered by these planes parallel with the surface [9]. The basal planes have the highest binding energy of the surface atoms and the total energy involved in the breaking of the bonds and the subsequent dissolution of atoms is highest for these planes [10].

In other words, surface becomes electrochemically less active due to surface energy which value is inversely proportional to the atomic spacing (d), and is lowest for basal plane with respect to other planes in hcp structure (for example: 1/d = 0.41; 0.89 and 0.85 for (00.2), (20.1) and (11.2) planes, respectively). Because of this excellent dissolution resistance, coating with higher relative intensity of (00.2) basal texture component will be corroded much slower than those of lower relative intensity of (00.2) basal texture component [9-10].

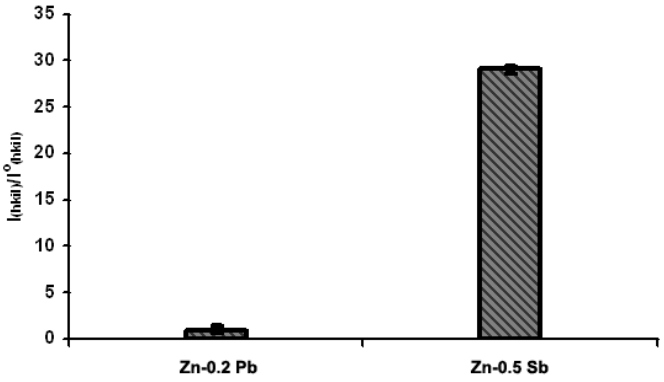

Fig.4. Effects of Pb and Sb content of zinc bath on the (00.2) basal texture component

The behavior of Zn-0.2 Pb and Zn-0.5 Sb coatings was evaluated using potentiodynamic polarization technique. Typical polarization curves of these coatings obtained in 3.5 wt.% NaCl solution are shown in Figure 5. The results show that Zn-0.2 Pb coatings as well as Zn-0.5 Sb exhibit lower corrosion potential (E_{corr}), which is good enough for sacrificial cathodic protection, in the presence of aqueous electrolyte. Zn-0.2 Pb coating exhibits higher corrosion current density (i_{corr}) than that of Zn-0.2 Pb coating. This means that the increase in corrosion resistance, due to Pb addition, may be the consequence of the resistance in anodic dissolution of the coating. The cathodic Tafel slope is very low compared to what is expected from a diffusion controlled reaction. For the same reason, the cathodic curve does not show the limiting current. In general, the limiting current decreases as the corrosion products are deposited on the electrode surface, which restricts the supply of oxygen to the cathodic area [11].

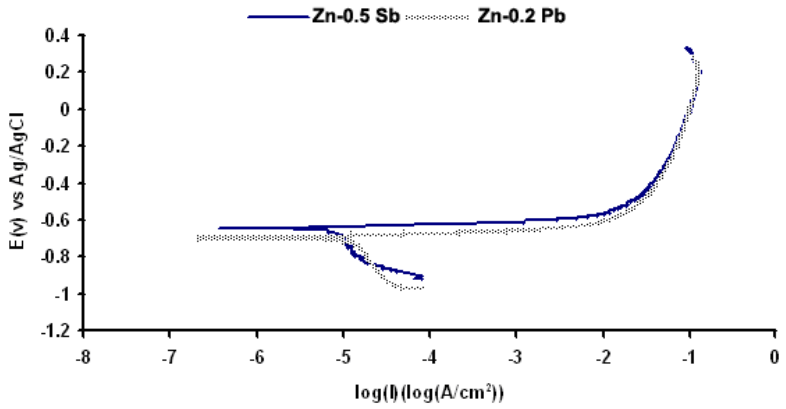

Fig.5. Potentiodynamic polarization curves of hot-dip galvanized coating obtained in 3.5 wt.% NaCl

Figures 6 and 7, illustrate the evolution of the impedance diagrams for the Zn-0.2 Pb and Zn-0.5 Sb coatings, respectively, as a function of the immersion time in 3.5% NaCl aqueous solution, with the characteristic frequencies indicated in each Nyquist diagram. The Nyquist diagram of the Zn-0.2 Pb coating immersed for 1 h shows three loops (Figure 6). The existence of three loops in the Nyquist diagrams obtained for Zn in sulfate and chloride aerated media has been reported by other authors [12] and are in close agreement with the results presented here. Thus, the capacitive loop in the high frequency range is attributed to the first charge transfer resistance (R_{ct}) in parallel with the double layer capacitance (C_{dl}), whose value is 208 μF cm^{-2}. The second capacitive loop, which had a characteristic frequency of 0.1993 Hz, was related to intermediate charge transfer adsorption, while the inductive loop, with a characteristic frequency of 0.0243 Hz, was associated with the coverage relaxation of adsorbed species such as Zn^{+}, Zn^{2+} and $(ZnOH)_{ads}$. With longer immersion times, the impedance diagrams evolved to

two capacitive loops, showing a Warburg diffusion component on 5 day of immersion, which is related to the diffusion of O_2 through the corrosion film [13].

The impedance diagrams of the Zn-0.5 Sb immersed for 1 hour showed one capacitive loop in the high frequency range corresponding to the electron transfer reaction at the metal/solution interface presenting a capacitive value of 140 μF cm^{-2} and 520 mF cm^{-2}, respectively, and a second loop in the low frequency range. For 1 day of immersion, the impedance diagram of the Zn-0.5 Sb coating presented a partially resolved semicircle in the high frequency range, followed by a Warburg diffusion component in the low frequency range, while for longer immersion times the impedance diagrams of this sample evolved to two partially resolved capacitive arcs. This feature is typical of a surface containing corrosion products acting as a barrier against corrosion, which was confirmed by the SEM analysis However, the presence of these corrosion products on the surface did not prevent the evolution of the corrosion process of the Zn-0.5 Sb coating [14-16].

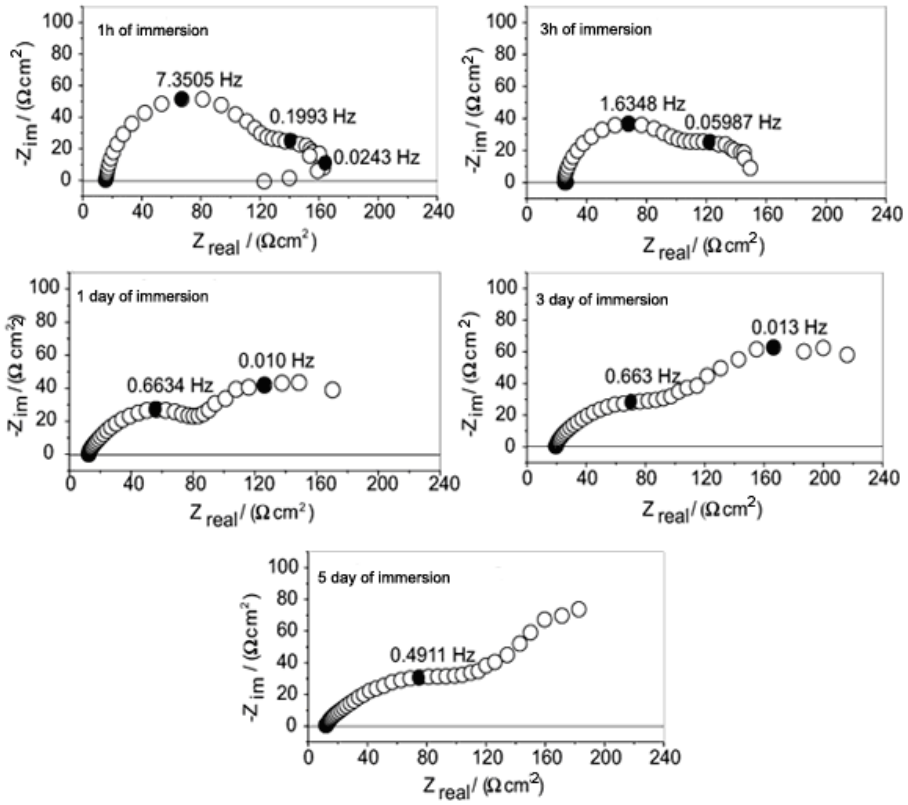

Fig.6. Evolution of the impedance diagrams with immersion time of Zn-0.2 Pb in 3.5 wt.% NaCl aqueous solution at room temperature

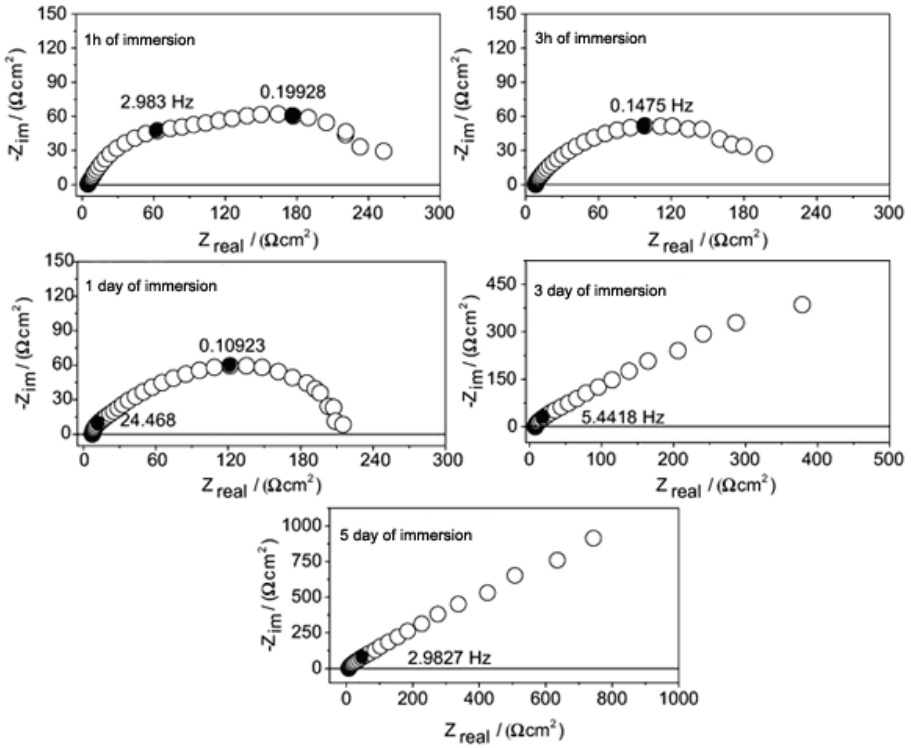

Fig.7. Evolution of the impedance diagrams with immersion time of Zn-0.5 Sb in 3.5 wt.% NaCl aqueous solution at room temperature

Conclusions

From the results presented in this paper, the following conclusions can be drawn:

Addition of Pb in the zinc bath would results in decrease of (00.2) basal texture component relative intensity. Also adding Sb decreased (00.2) basal texture component in comparison with pure zinc, but the effect of Pb is more harmful. The corrosion mechanism of Zn coatings with Sb content in the zinc bath is related to the appearance of cracks in response to the dissolution of γ Zn-rich phases. On the other hand, the corrosion mechanism of Zn coatings with Pb content in the zinc bath was characterized by the local dissolution of the coatings and decreasing of (00.2) basal texture component. The same insoluble corrosion products, which act as a barrier against corrosion but do not prevent it, were identified on Zn coatings in the both cases. The better corrosion resistance of the Zn-0.5 Sb coating is due to high Sb content, which leads to an ennoblement of the coating and stronger (00.2) basal texture component compare with Zn-0.2 Pb coating.

References

[1] A.R. Marder, Prog. Mater. Sci. 45 (2000) 271-191.
[2] S. Changa and J.C. Shin, Corr. Sci. 36 (1994) 1425-1436.
[3] E. Pavlidou, N. Pistofidis, G. Vourlias, Mat. Letters 59 (2005) 1619– 1622.
[4] J. Elvins, J.A. Spittle, Corr. Sci. 47 (2005) 2740–2759.
[5] A. E. Shiel, D. Weis, K.J. Orians, Sci.Tot.Env, 408 (2010) 2357–2368.
[6] H. Park, J. A. Szpunar, Corr.Sci. 40 (1998) 525-545.
[7] A. Chakraborty, R.K. Ray, Surf. Coat. Technol. 203 (2009) 1756–1764.
[8] Evangelos Tzimas, George Papadimitriou, Surf. Coat. Technol. 145 (2001) 176-185.
[9] H. Asgari, M.R. Toroghinejad, M.A. Golozar, Curr. Appl. Phys. 9 (2007) 6777-6769.
[10] H. Asgari, M.R. Toroghinejad, M.A. Golozar, ISIJ. 48 (2008) 628-633.
[11] Zhiyi Yong, Jin Zhu, Cheng Qiu, Yali Liu, Curr. Appl. Phys. 255 (2008) 1672–1680.
[12] Y. Hamlaoui, F . Pedraza , L. Tifouti, Ame.Jour.Appl.Sci. 7 (2007) 430-438.
[13] E. Barsoukov, J. Ross Macdonald, Impedance Spectroscopy Theory, Experiment, and Applications, second ed., John Wiley & Sons, New Jersey, 2005.
[14] S.Lee, S, Pyun, J. Solid. State. Electrochem. 11 (2007) 829–839.
[15] K. Darowicki, J. Orlikowski, A. Arutunow, Electrochimica.Acta. 48 (2003) 4189–4196.
[16] F. Rosalbino, E. Angelini, D. Macci, A. Saccone, S. Delfino, Electrochimica.Acta. 54 (2009) 1204–1209.